

Supplementary File for

**Reactivation Potential of Intraplate Faults in the Western Quebec Seismic Zone, Eastern Canada**

Jeremy Rimando<sup>1</sup>, Alexander Peace<sup>1</sup>

<sup>1</sup>School of Earth, Environment and Society, McMaster University, Hamilton, Ontario, Canada

\*Corresponding author: [rimandoj@mcmaster.ca](mailto:rimandoj@mcmaster.ca)

### **Contents of this file**

Figures S1 to S4

Table S1

### **Introduction**

This supplementary file includes maps of the reactivation potential of faults in the WQSZ (for SH azimuths of 28° and 73°) modelled using the 'Stress Analysis' module of the software Move™ by Petroleum Experts Limited (<https://www.petex.com/>), and the software 'Slicken 1.0' by Xu et al. (2017) (<https://doi.org/10.1016/j.cageo.2016.07.015>).

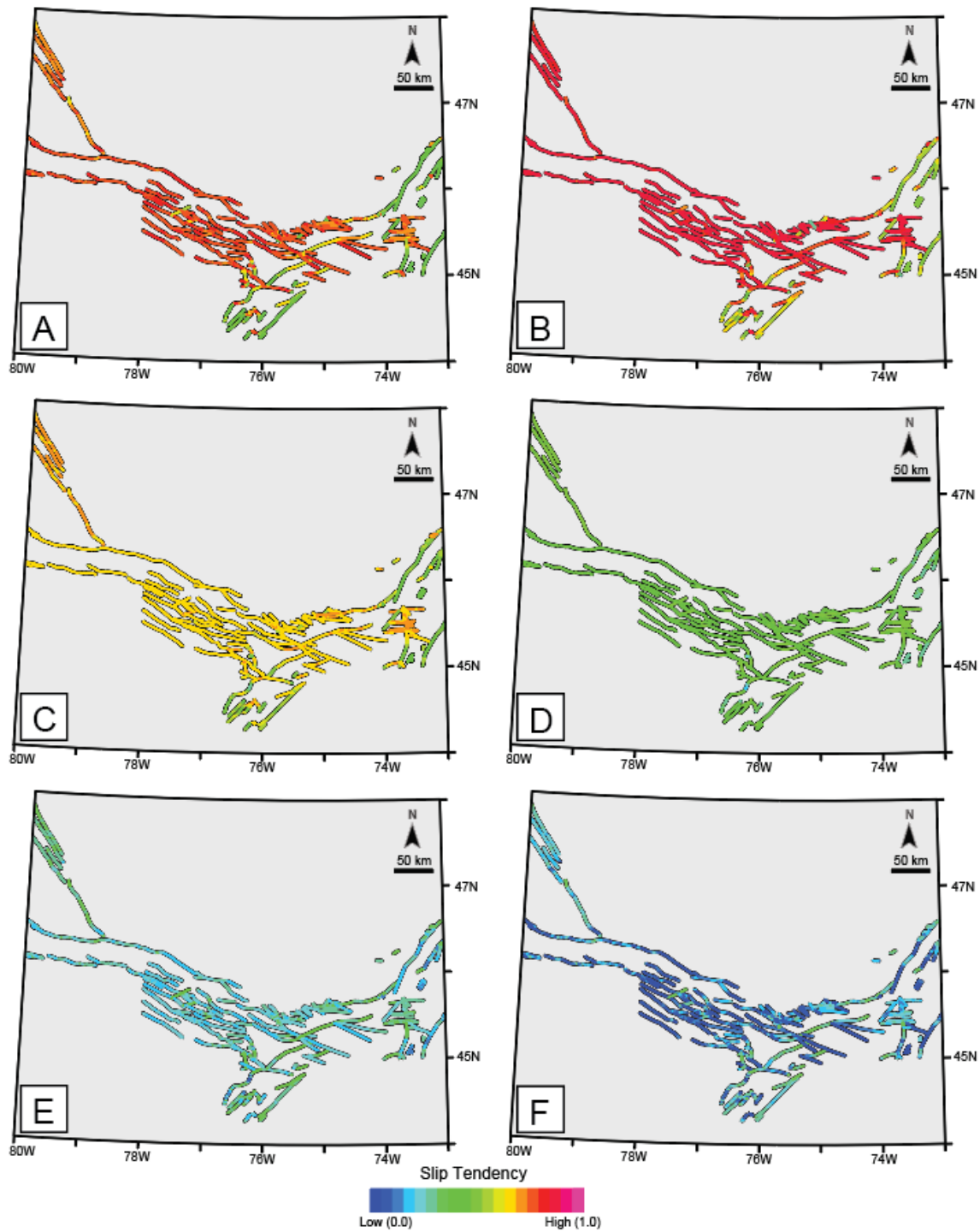


**Figure S1.** Slip tendency maps for different fault dip scenarios (with an  $S_H$  azimuth of  $28^\circ$ ). **A)**  $15^\circ$ , **B)**  $30^\circ$ , **C)**  $45^\circ$ , **D)**  $60^\circ$ , **E)**  $75^\circ$ , and **F)**  $90^\circ$ .

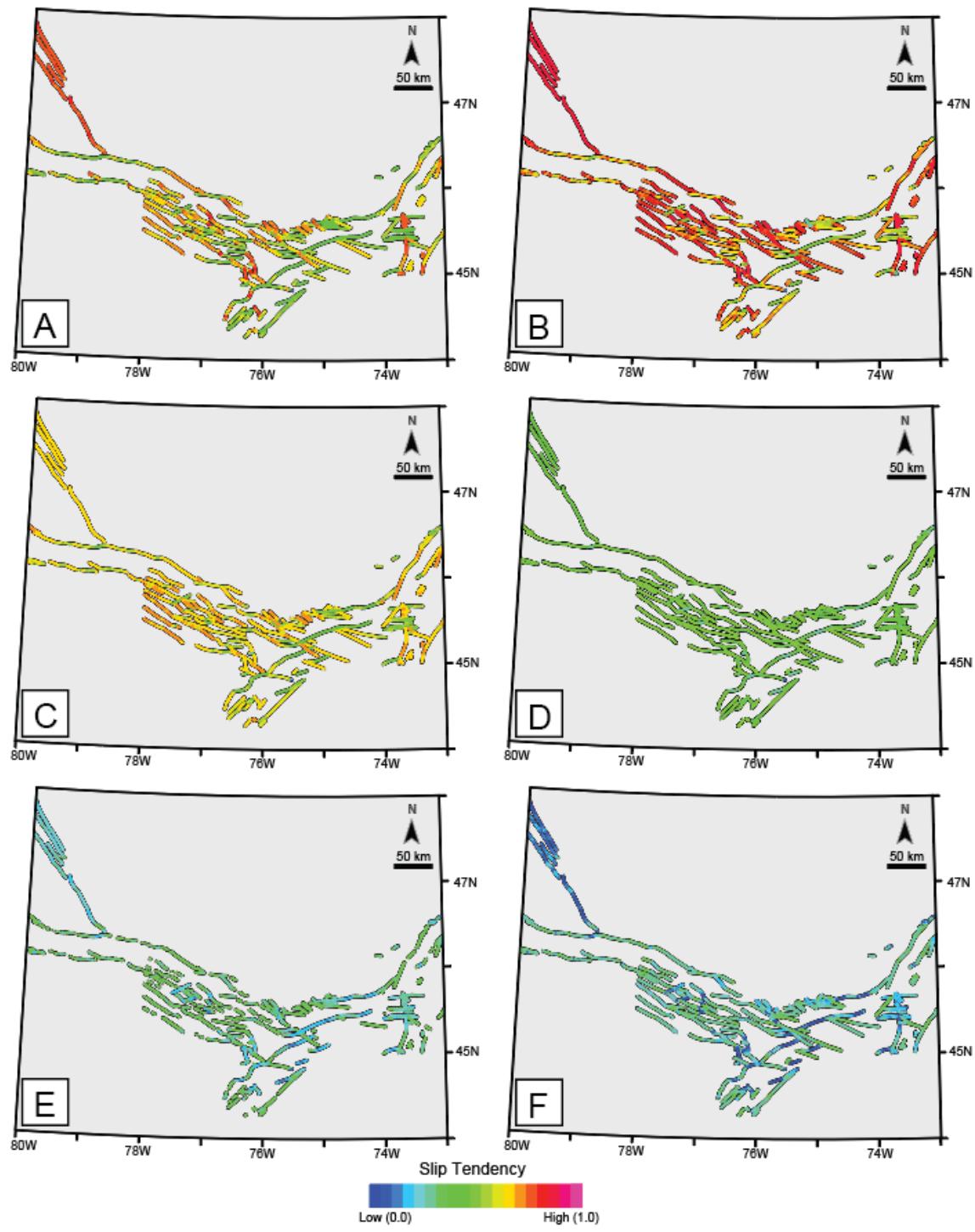


**Figure S2.** Slip tendency maps for different fault dip scenarios (with an  $S_H$  azimuth of  $73^\circ$ ). **A)**  $15^\circ$ , **B)**  $30^\circ$ , **C)**  $45^\circ$ , **D)**  $60^\circ$ , **E)**  $75^\circ$ , and **F)**  $90^\circ$ .

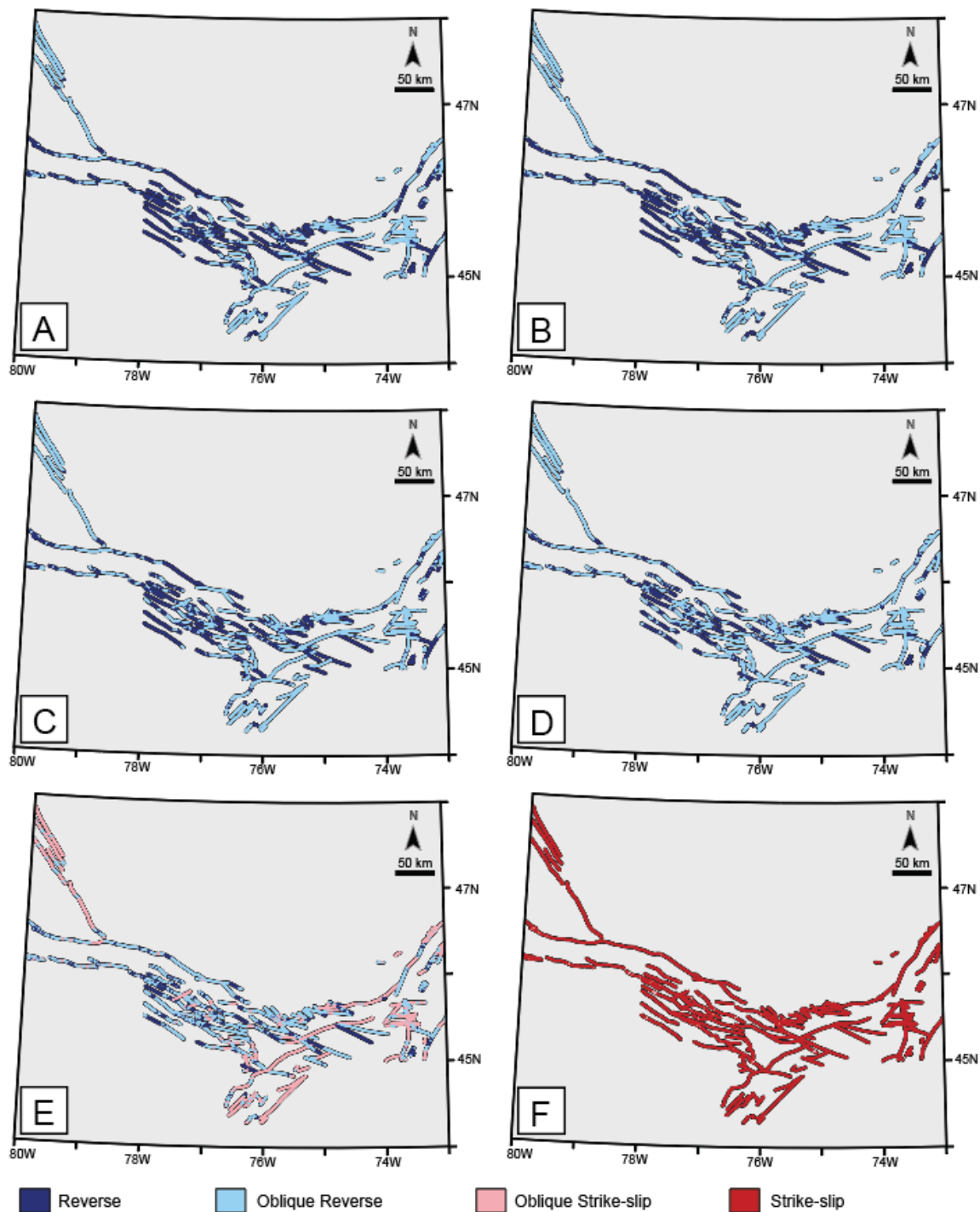


**Figure S3.** Predicted slip kinematics for different fault dip scenarios (with an  $S_H$  azimuth of  $28^\circ$ ).  
**A)**  $15^\circ$ , **B)**  $30^\circ$ , **C)**  $45^\circ$ , **D)**  $60^\circ$ , **E)**  $75^\circ$ , and **F)**  $90^\circ$ .

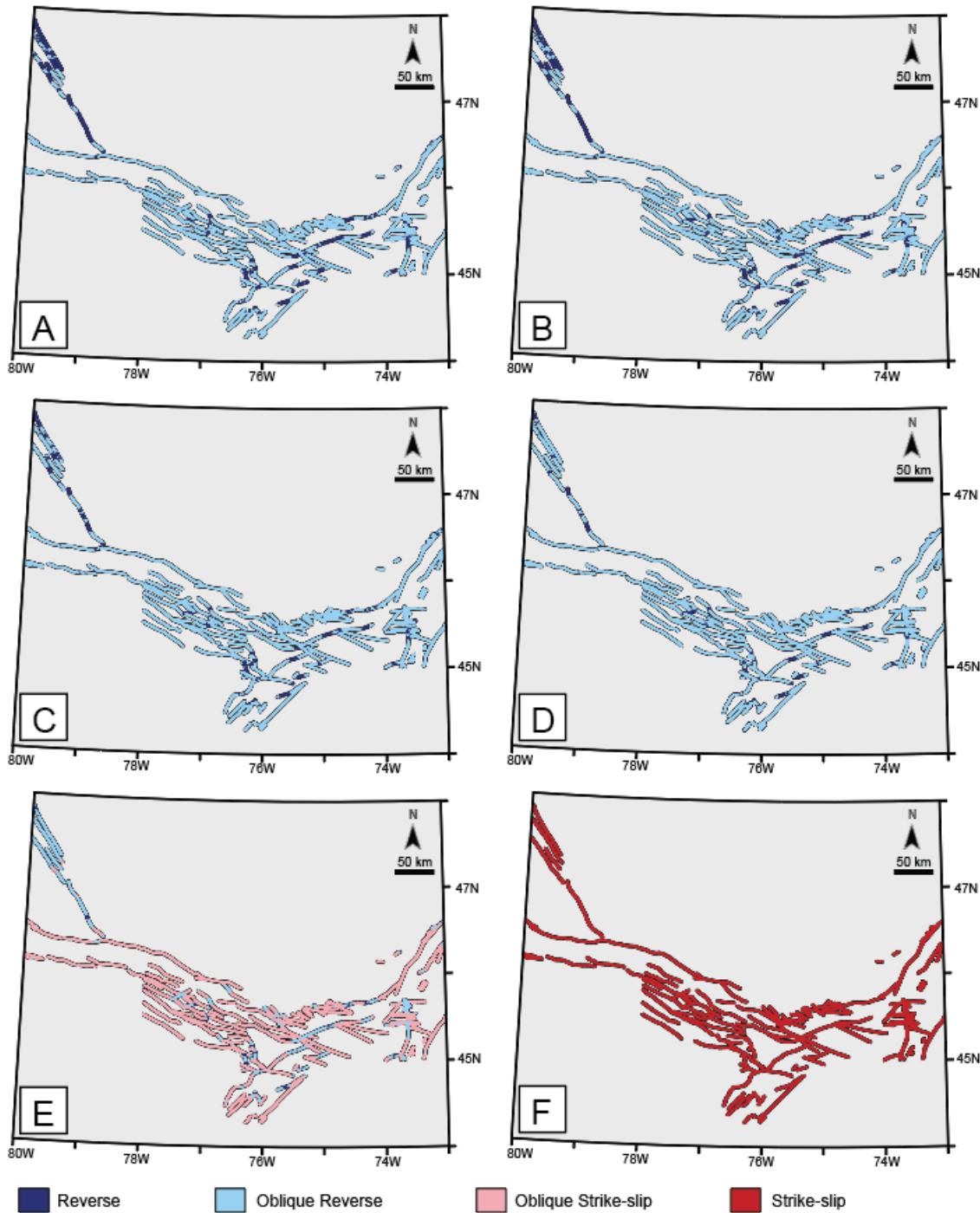


**Figure S4.** Predicted slip kinematics for different fault dip scenarios (with an  $S_H$  azimuth of  $73^\circ$ ). **A)**  $15^\circ$ , **B)**  $30^\circ$ , **C)**  $45^\circ$ , **D)**  $60^\circ$ , **E)**  $75^\circ$ , and **F)**  $90^\circ$ .

$\sigma_1$ Azimuth	Fault Dip	Slip tendency							
		NW-striking faults				NE-striking faults			
		Mean	Std. Dev.	Min	Max	Mean	Std. Dev.	Min	Max
28°	15°	0.78	0.00	0.34	0.90	0.55	0.00	0.37	0.83
	30°	0.86	0.00	0.25	0.87	0.69	0.00	0.41	0.85
	45°	0.67	0.00	0.33	0.69	0.60	0.00	0.31	0.69
	60°	0.45	0.00	0.26	0.52	0.44	0.00	0.20	0.52
	75°	0.25	0.00	0.15	0.39	0.30	0.00	0.10	0.39
	90°	0.12	0.00	0.00	0.33	0.23	0.00	0.00	0.33
45°	15°	0.76	0.00	0.27	0.88	0.50	0.00	0.37	0.76
	30°	0.85	0.00	0.13	0.87	0.64	0.00	0.41	0.81
	45°	0.68	0.00	0.25	0.69	0.57	0.00	0.28	0.69
	60°	0.46	0.00	0.20	0.52	0.43	0.00	0.18	0.52
	75°	0.28	0.00	0.13	0.37	0.30	0.00	0.11	0.39
	90°	0.17	0.00	0.00	0.32	0.23	0.00	0.00	0.33
73°	15°	0.64	0.00	0.08	0.88	0.49	0.00	0.37	0.88
	30°	0.77	0.00	0.06	0.87	0.63	0.00	0.39	0.86
	45°	0.65	0.00	0.06	0.69	0.56	0.00	0.29	0.69
	60°	0.48	0.00	0.05	0.52	0.49	0.00	0.23	0.52
	75°	0.34	0.00	0.03	0.39	0.29	0.00	0.14	0.39
	90°	0.27	0.00	0.00	0.33	0.22	0.00	0.00	0.33

**Table S1.** Average slip tendency values for different  $\sigma_1$  azimuths and fault dips.